diversity

MDPI

Article

Translation Elongation Factor 1-Alpha Sequencing Provides Reliable Tool for Identification of *Fusarium graminearum* Species Complex Members

Emre Yörük [1] and Tapani Yli-Mattila [2,*]

[1] Department of Molecular Biology and Genetics, Faculty of Sciences and Literature, Istanbul Yeni Yuzyil University, Cevizlibag, Istanbul 34010, Turkey; emre.yoruk@yeniyuzyil.edu.tr
[2] Department of Life Technologies, Molecular Plant Biology, University of Turku, FI-20520 Turku, Finland
* Correspondence: tymat@utu.fi; Tel.: +358-44-0560700

Abstract: The *Fusarium graminearum* species complex (FGSC) is a worldwide phytopathogenic fungus of small grain cereals. Genetics and bioinformatics tools have been providing an efficient strategy for identifying FGSC. However, the potential reliability of *tef1−α* sequencing in FGSC members has not been well investigated. In this study, the *tef1−α* sequencing data of 246 FGSC members, one *F. culmorum*, and one *F. solani* isolate were subjected to distance-, character-, and PCA-based phylogenetic analysis. Linux terminals and the R programming language were used in phylogenetic analysis. The Unweighted Pair Group Method with Arithmetic Mean (UPGMA) and maximum likelihood methods produced relatively more homogenous *F. graminearum sensu stricto* (*Fgss*) and *F. asiaticum* isolates. *Fgss* and *F. asiaticum* isolates co-clustered in two separate sub-divisions in the ML and UPGMA methods, with significant differences in the Chi2 test ($p < 0.05$). PCA profiling revealed a low level of variation in FGSC members, with 99–99.5% percentages in axis 1. An increased number of taxa and isolates would be tested for *tef1−α* in future studies. To our knowledge, this is also the first study to combine phylogenetic methods with PCA tests for comprehensive characterization of FGSC members.

Keywords: DNA sequencing; *Fusarium graminearum*; PCR; phylogenetics; *tef1−α*

check for updates

Citation: Yörük, E.; Yli-Mattila, T. Translation Elongation Factor 1-Alpha Sequencing Provides Reliable Tool for Identification of *Fusarium graminearum* Species Complex Members. *Diversity* **2024**, *16*, 481. https://doi.org/10.3390/d16080481

Academic Editor: Ipek Kurtboke

Received: 15 July 2024
Revised: 4 August 2024
Accepted: 5 August 2024
Published: 8 August 2024

Copyright: © 2024 by the authors. Licensee MDPI, Basel, Switzerland. This article is an open access article distributed under the terms and conditions of the Creative Commons Attribution (CC BY) license (https://creativecommons.org/licenses/by/4.0/).

1. Introduction

Fusarium graminearum, a phytopathogenic fungus, is a major concern in agriculture due to its ability to cause destructive diseases in small grain cereals, especially wheat, barley, and maize [1–3]. This phytopathogenic fungus has been reported as a major causal agent of Fusarium head blight (FHB) and crown rot (CR) diseases in many geographic regions worldwide. Moreover, *F. graminearum* could produce B-type trichothecenes, zearalenone, and some other mycotoxins, which are not only hazardous for plants but also for humans and animals [4,5]. This species has been reported as one of the top 10 phytopathogenic fungi worldwide [6].

Over the last two decades, this species has been announced and accepted as a species complex, the *F. graminearum* species complex (FGSC), which includes more than ten members. *Fgss* (*Fgss*) and *F. asiaticum* seem to be the predominant members of the FGSC. Members present differences in chemotypes, geographic distribution, and morphological characteristics [3,7]. Accurate identification of the members within FGSC is crucial for developing effective disease management strategies.

Sequence-characterized amplified marker (SCAR)-based identification of *F. graminearum* was historically very important in terms of distinguishing the FGSC from other FHB and CR agents [8–10]. Especially UBC85 and FG16 SCARs have been widely used in species-specific characterization and identification of *F. graminearum* isolates worldwide [8,9]. However, the lineage characterization of the FGSC in the early 2000s led

scientists to use detailed characterization protocols. Fortunately, the development of more effective DNA sequencing platforms and whole genome sequencing technologies has made it easier for researchers. These platforms and strategies, including gene-specific or genome-wide sequencing data, yielded fast and reliable results within a short time period. In this way, single- or multip-copy gene sequencing, merging conserved DNA sequences as a multilocus, and the alignment of these sequences provided another aspect of FGSC characterization [11–15]. Translation elongation factor 1-α (*tef1−α*: FG08811), α-tubulin (*α-tub*: FG00639), histone H3 (*HIS:* FG04290), mating type locus (*MAT:* FG08890-93), β-tubulin (*β-tub*: FG09530), reductase (*RED*: FG03224), phosphate permease (*PHO:* FG07894), trichothecene 3-O-acetyltransferase (*TRI101*: FG07896), and ammonium ligase (*URA*: FG07897) genes have been widely used for obtaining detailed FGSC member identification by multilocus sequencing and/or genealogical concordance analysis by using probe-based identification assays. Additionally, ITS/28S rDNA, as multi-copy regulatory RNA coding regions, has been used in multilocus assays for FGSC member identification [14,15]. It could be concluded that so far the geographic region, chemotype, aggressiveness, and morphologically distinct characteristics of FGSC members have been well characterized by using sequencing and/or probe-based real time identification techniques.

One approach that has gained great importance in recent years is the use of *tef1−α* as a genetic marker for the identification of members within the FGSC. *tef1−α* is a highly conserved protein that plays a crucial role in protein synthesis, making it a potentially reliable target for species differentiation [7,11–13]. DNA sequencing and/or probe-based hybridization methods could accurately distinguish members within the complex. It could be clearly seen that plenty of scientific reports, including those involving FGSC members (mainly *Fgss*), revealed FGSC member identification by only *tef1−α* DNA sequencing [16,17]. Due to the non-monophylogenetic structure of FGSC, single gene sequencing-based molecular identification methods could reveal inaccurate results, such as in SCAR-based identification methods [18–20]. Thus, the efficiency and/or reliability of *tef1−α* for accurate FGSC member identification should be tested. In this study, the aim was to reveal the potential reliability of *tef1−α* sequencing in FGSC member identification by distance-based and character-based phylogenetic analysis. Presenting the potential reliability of *tef1−α* sequencing as a single locus in comparison to multilocus sequencing investigations could accelerate the rate of genetic characterization studies of FGSC worldwide.

2. Materials and Methods

2.1. FGSC Isolate Sequences, Format Converting, and Preparing Samples for Alignment

F. graminearum, as a species complex, includes 15 members with accession numbers deposited under GenBank for specific gene sequences. Fourteen members with accession numbers provided for *tef1−α* gene sequences were used in the phylogenetic analysis. In total, 246 *tef1−α* gene sequences for FGSC members were obtained as ".fasta" files from GenBank. 100 and 92 of these sequences belonged to *Fgss* and *F. asiaticum*, respectively (Table 1). *tef1−α* gene sequences with accession number OQ876777 of *F. culmorum* (causing head blight and crown rot but not belonging to FGSC) were used for internal control of phylogenetic analysis. Similarly, *tef1−α* gene sequences with accession number MG183712 of *F. solani* (not causal agents of head blight or crown rot) were used as an external control in phylogenetic analysis.

Labels from "A_" to "P_" (such as OP245201, which is edited as A_OP245201 for the *F. acacia-mearnsii tef1−α* accession) were placed just before the accession numbers of sequences to easily follow of samples in phylogenetic trees (Table 1). "Extract" and "export table" functions of Phylosuite software (v1.2.3) were used to construct a table including accession numbers. The "cat" function from the Linux terminal was used to obtain three separate aligned fasta files. These three aligned files formed three sample sets:

(i) The first of these three aligned ".fasta" files, named Set I, included *F. asiaticum* alignment with 107 isolates (not containing *Fgss*).

(ii) The second one, named Set II, included *Fgss* alignment with 115 isolates (not containing *F. asiaticum*).
(iii) The third one, named Set III, included all 248 isolates.

After basic alignment using MAFFT software (version 7), ".aln" files were obtained, and these aligned files were converted to ".phy" and ".nexus" formats using the online tool lirmm.fr (please see https://www.lirmm.fr, accessed on 25 May 2024).

Table 1. FGSC isolates subjected to phylogenetic analysis in this study with their accession numbers.

No	Species	Sample Code	No	Species	Sample Code	No	Species	Sample Code	No	Species	Sample Code
1	*F. acacia-mearnsii*	A_OP245201	63	*F. asiaticum*	C_KY466730	125	*Fgss*	J_OR440886	187	*Fgss*	J_OR440824
2	*F. acacia-mearnsii*	A_MW233086	64	*F. asiaticum*	C_KY466706	126	*Fgss*	J_OR440885	188	*Fgss*	J_OR440823
3	*F. aethiopicum*	B_ON601768	65	*F. asiaticum*	C_KY283938	127	*Fgss*	J_OR440884	189	*Fgss*	J_OR440822
4	*F. aethiopicum*	B_MW233126	66	*F. asiaticum*	C_KY283936	128	*Fgss*	J_OR440883	190	*Fgss*	J_OR440821
5	*F. asiaticum*	C_LC489415	67	*F. asiaticum*	C_KY283930	129	*Fgss*	J_OR440882	191	*Fgss*	J_OR440820
6	*F. asiaticum*	C_LC500695	68	*F. asiaticum*	C_KY283929	130	*Fgss*	J_OR440881	192	*Fgss*	J_OR440819
7	*F. asiaticum*	C_MW233069	69	*F. asiaticum*	C_KY283927	131	*Fgss*	J_OR440879	193	*Fgss*	J_OR689619
8	*F. asiaticum*	C_OM721590	70	*F. asiaticum*	C_KY283926	132	*Fgss*	J_OR440880	194	*Fgss*	J_OR689618
9	*F. asiaticum*	C_MH448758	71	*F. asiaticum*	C_KY283925	133	*Fgss*	J_OR440878	195	*Fgss*	J_MN308186
10	*F. asiaticum*	C_MH448757	72	*F. asiaticum*	C_KY283924	134	*Fgss*	J_OR440877	196	*Fgss*	J_MF974407
11	*F. asiaticum*	C_MH448756	73	*F. asiaticum*	C_KY283922	135	*Fgss*	J_OR440876	197	*Fgss*	J_LC796865
12	*F. asiaticum*	C_MH448755	74	*F. asiaticum*	C_KY283917	136	*Fgss*	J_OR440875	198	*Fgss*	J_LC796848
13	*F. asiaticum*	C_MH448754	75	*F. asiaticum*	C_KY283915	137	*Fgss*	J_OR440874	199	*Fgss*	J_LC796847
14	*F. asiaticum*	C_MH448753	76	*F. asiaticum*	C_KY283912	138	*Fgss*	J_OR440873	200	*Fgss*	J_OR529761
15	*F. asiaticum*	C_MH448752	77	*F. asiaticum*	C_KY283907	139	*Fgss*	J_OR440872	201	*Fgss*	J_OR528697
16	*F. asiaticum*	C_MH448751	78	*F. asiaticum*	C_KY283905	140	*Fgss*	J_OR440871	202	*Fgss*	J_OR528696
17	*F. asiaticum*	C_MH448750	79	*F. asiaticum*	C_KY283903	141	*Fgss*	J_OR440870	203	*Fgss*	J_OR528695
18	*F. asiaticum*	C_MH448749	80	*F. asiaticum*	C_KY283895	142	*Fgss*	J_OR440869	204	*Fgss*	J_OR528694
19	*F. asiaticum*	C_MH448748	81	*F. asiaticum*	C_KY283886	143	*Fgss*	J_OR440868	205	*Fgss*	J_OR528693
20	*F. asiaticum*	C_KY466790	82	*F. asiaticum*	C_KY283888	144	*Fgss*	J_OR440867	206	*Fgss*	J_OR424554
21	*F. asiaticum*	C_KY466787	83	*F. asiaticum*	C_KY283885	145	*Fgss*	J_OR440866	207	*Fgss*	J_OR424551
22	*F. asiaticum*	C_KY466786	84	*F. asiaticum*	C_KY283879	146	*Fgss*	J_OR440865	208	*Fgss*	J_OR424549
23	*F. asiaticum*	C_KY466785	85	*F. asiaticum*	C_KY283877	147	*Fgss*	J_OR440864	209	*Fgss*	J_OR424548
24	*F. asiaticum*	C_KY466784	86	*F. asiaticum*	C_KY283876	148	*Fgss*	J_OR440863	210	*Fgss*	J_OR424546
25	*F. asiaticum*	C_KY466782	87	*F. asiaticum*	C_KY283875	149	*Fgss*	J_OR440862	211	*Fgss*	J_OR424541
26	*F. asiaticum*	C_KY466781	88	*F. asiaticum*	C_KY283874	150	*Fgss*	J_OR440861	212	*Fgss*	J_OR424540
27	*F. asiaticum*	C_KY466778	89	*F. asiaticum*	C_KY283862	151	*Fgss*	J_OR440860	213	*Fgss*	J_OQ925578
28	*F. asiaticum*	C_KY466777	90	*F. asiaticum*	C_KY283867	152	*Fgss*	J_OR440859	214	*Fgss*	J_OQ925577
29	*F. asiaticum*	C_KY466776	91	*F. asiaticum*	C_KY283861	153	*Fgss*	J_OR440858	215	*F. meridionale*	K_PP034521
30	*F. asiaticum*	C_KY466775	92	*F. asiaticum*	C_KX702562	154	*Fgss*	J_OR440857	216	*F. meridionale*	K_MW233092
31	*F. asiaticum*	C_KY466771	93	*F. asiaticum*	C_KX702559	155	*Fgss*	J_OR440856	217	*F. meridionale*	K_MG838991
32	*F. asiaticum*	C_KY466770	94	*F. asiaticum*	C_DQ295124	156	*Fgss*	J_OR440855	218	*F. meridionale*	K_MG838988
33	*F. asiaticum*	C_KY466769	95	*F. asiaticum*	C_DQ295123	157	*Fgss*	J_OR440854	219	*F. meridionale*	K_MG838955
34	*F. asiaticum*	C_KY466768	96	*F. asiaticum*	C_HQ214263	158	*Fgss*	J_OR440853	220	*F. meridionale*	K_MG838949
35	*F. asiaticum*	C_KY466767	97	*F. austroamericanum*	D_MW233095	159	*Fgss*	J_OR440852	221	*F. meridionale*	K_MG838948
36	*F. asiaticum*	C_KY466766	98	*F. boothii*	E_OP245207	160	*Fgss*	J_OR440851	222	*F. meridionale*	K_MG838947
37	*F. asiaticum*	C_KY466765	99	*F. boothii*	E_OP245206	161	*Fgss*	J_OR440850	223	*F. meridionale*	K_MH448800
38	*F. asiaticum*	C_KY466764	100	*F. boothii*	E_OP245205	162	*Fgss*	J_OR440849	224	*F. meridionale*	K_MH448801
39	*F. asiaticum*	C_KY466763	101	*F. boothii*	E_OP245204	163	*Fgss*	J_OR440848	225	*F. meridionale*	K_MH448802
40	*F. asiaticum*	C_KY466762	102	*F. boothii*	E_PP035520	164	*Fgss*	J_OR440847	226	*F. meridionale*	K_MH448803
41	*F. asiaticum*	C_KY466761	103	*F. boothii*	E_PP035519	165	*Fgss*	J_OR440846	227	*F. meridionale*	K_MH448796
42	*F. asiaticum*	C_KY466760	104	*F. boothii*	E_ON601969	166	*Fgss*	J_OR440845	228	*F. meridionale*	K_MH448797
43	*F. asiaticum*	C_KY466759	105	*F. boothii*	E_ON601968	167	*Fgss*	J_OR440844	229	*F. meridionale*	K_MH448798
44	*F. asiaticum*	C_KY466757	106	*F. boothii*	E_ON601967	168	*Fgss*	J_OR440843	230	*F. meridionale*	K_MH448799
45	*F. asiaticum*	C_KY466758	107	*F. boothii*	E_MW233088	169	*Fgss*	J_OR440842	231	*F. meridionale*	K_KY466783
46	*F. asiaticum*	C_KY466756	108	*F. boothii*	E_KY794904	170	*Fgss*	J_OR440841	232	*F. meridionale*	K_KY466779
47	*F. asiaticum*	C_KY466755	109	*F. brasilicum*	F_MW233104	171	*Fgss*	J_OR440840	233	*F. meridionale*	K_KY466774
48	*F. asiaticum*	C_KY466754	110	*F. cortaderiae*	G_MW233098	172	*Fgss*	J_OR440839	234	*F. meridionale*	K_KY466773
49	*F. asiaticum*	C_KY466752	111	*F. cortaderiae*	G_MT193123	173	*Fgss*	J_OR440838	235	*F. meridionale*	K_KY466772
50	*F. asiaticum*	C_KY466751	112	*F. cortaderiae*	G_MT193124	174	*Fgss*	J_OR440837	236	*F. meridionale*	K_KY466735
51	*F. asiaticum*	C_KY466749	113	*F. culmorum*	H_OQ876777	175	*Fgss*	J_OR440836	237	*F. meridionale*	K_KY466733

Table 1. *Cont.*

No	Species	Sample Code	No	Species	Sample Code	No	Species	Sample Code	No	Species	Sample Code
52	*F. asiaticum*	C_KY466747	114	*F. gerlachii*	I_MW233118	176	*Fgss*	J_OR440835	238	*F. meridionale*	K_KY466732
53	*F. asiaticum*	C_KY466746	115	*Fgss*	J_OR440896	177	*Fgss*	J_OR440834	239	*F. meridionale*	K_KY466731
54	*F. asiaticum*	C_KY466744	116	*Fgss*	J_OR440895	178	*Fgss*	J_OR440833	240	*F. meridionale*	K_KY466718
55	*F. asiaticum*	C_KY466743	117	*Fgss*	J_OR440894	179	*Fgss*	J_OR440832	241	*F. meridionale*	K_HQ214262
56	*F. asiaticum*	C_KY466740	118	*Fgss*	J_OR440893	180	*Fgss*	J_OR440831	242	*F. mesoameri-canum*	L_MW233083
57	*F. asiaticum*	C_KY466741	119	*Fgss*	J_OR440892	181	*Fgss*	J_OR440830	243	*F. nepalense*	M_MW233135
58	*F. asiaticum*	C_KY466739	120	*Fgss*	J_OR440891	182	*Fgss*	J_OR440829	244	*F. solani*	N_MG183712
59	*F. asiaticum*	C_KY466738	121	*Fgss*	J_OR440890	183	*Fgss*	J_OR440828	245	*F. ussurianum*	O_MW233125
60	*F. asiaticum*	C_KY466737	122	*Fgss*	J_OR440889	184	*Fgss*	J_OR440826	246	*F. vorosii*	P_MW233119
61	*F. asiaticum*	C_KY466736	123	*Fgss*	J_OR440888	185	*Fgss*	J_OR440827	247	*F. vorosii*	P_KY586243
62	*F. asiaticum*	C_KY466734	124	*Fgss*	J_OR440887	186	*Fgss*	J_OR440825	248	*F. vorosii*	P_MF974401

2.2. Distance-Based Phylogenetic Methods

In total, three sample sets, Sets I, II, and III, were subjected to distance-based phylogenetic analysis. For the Unweighted Pair Group Method with Arithmetic Mean (UPGMA) and Neighbor Joining (NJ)-based phylogenetic analysis, FFT-NS-2, 200PAM/K = 2, Jukes–Cantor substitution modeling, and threshold score = 39 parameters were selected. Bootstrap support with 1000 hierarchical repeats was also used in NJ-based phylogenetic assays. Distance-based alignment produced a phylogenetic tree with Newick format, MSA profiling with conserved regions, plots, and ".aln" files. Phylogenetic trees were transferred to ITOL for visualization of dendrograms [21]. ITOL visualization parameters were as follows: circular tree mode with 210° rotation/350° arc, branch length usage, labels with accession numbers, no rotation, and separately colored sub-divisions.

2.3. Character-Based Phylogenetic Methods

Sample Sets I, II, and III were used in obtaining detailed phylogenetic analysis via character-based methods. For this purpose, maximum likelihood (ML) and Bayesian topology assays were carried out using iqtree (1.6.12) and MrBayes software (3.2.7a) on a Linux terminal (WSL2-based Ubuntu version 20.04). Aligned files with the ".phy" format were used in iqtree-based ML analysis [22]. The first command in the Linux terminal was "iqtree -s *filename*.phy" in order to obtain the best-fit model. Best-fit models were used in three different sample sets. The following command for bootstrapping and model selection was used in the Linux terminal: iqtree -s filename.phy -m modelname -bb 1000 -redo. ".tree" and ".phy" files, including base frequencies, site proportions, and rates, were obtained. The ".tree" file was transferred and processed using ITOL software (v6) as described above. For Bayesian topology analysis, MrBayes software was used using "nex/nexus" files [23]. For entering a bayesing window in the Linux terminal, the "mb" command was entered. Common sample size and rate-related commands were then followed as "execute *filename*.nex", "lset nst = 6 rates = invgamma", "mcmc ngen = 20,000 samplefreq = 100", "no *selection*", "sump", and "sumt". After finishing the Bayesian assay, tree files were processed and visualized using ITOL software.

2.4. Principal Component Analysis (PCA) by RStudio

PCA is a powerful strategy for visualizing and simplifying multiple experiments and/or data sets with a relatively high number of samples as a single holistic profile or figure. The potential relationship between *tef1*−*α* sequence differences and axis numbers and rates among FGSC members was figured out by PCA using "ape", "phangorn", "factoextra", and "readxl" packages in RStudio. ".phy" file was used in PCA processes. The distance matrix was obtained by describing a new variable, including the "dist.ml" function. After writing the distance matrix with the "readxl" package, new variables were characterized. "prcomp", "str", "fviz_eig", "rep" (with grouping with a specific number of

members), and "fviz_pca_ind" functions were used to obtain PCA graphics. Axis numbers and percentages were recorded for each sample set.

3. Results and Discussion

3.1. Distance-Based Phylogenetic Analysis

The aligned *tef1−α* sequences for three sets were obtained as different file types, including ".aln, .phy, and .nexus". The NJ dendrogram for Set I included five major clusters (Figure 1A). The majority of the samples appeared in four clusters that belonged to *F. asiaticum*. Only one cluster included only *F. asiaticum* samples. *F. culmorum* was located between two clusters, while *F. solani* clearly took quite a distant location compared to the majority of F. asiaticum samples. There was no perfectly homogenous distribution for the remaining FGSC members in the Set I NJ dendrogram. However, the Set II dendrogram obtained via NJ clustering produced a homogenous distribution for FGSC members, excluding *Fgss* (Figure 1B). Two clusters were present in the Set II NJ dendrogram and 83 of the 100 Fgss samples were included in cluster I. Cluster II included the remaining Fgss samples, *F. solani*, *F. culmorum*, and other FGSC members. The NJ dendrogram for Set III clearly distinguished two major FGSC members (*Fgss* and *F. asiaticum*), *F. boothii*, and *F. meridionale* (Figure S1). The Set III NJ dendrogram contained four major clusters, and two of them included *F. asiaticum* samples, while cluster I included *Fgss* samples. The remaining cluster is composed of the remaining FGSC members, primarily *F. boothii* and *F. meridionale* samples.

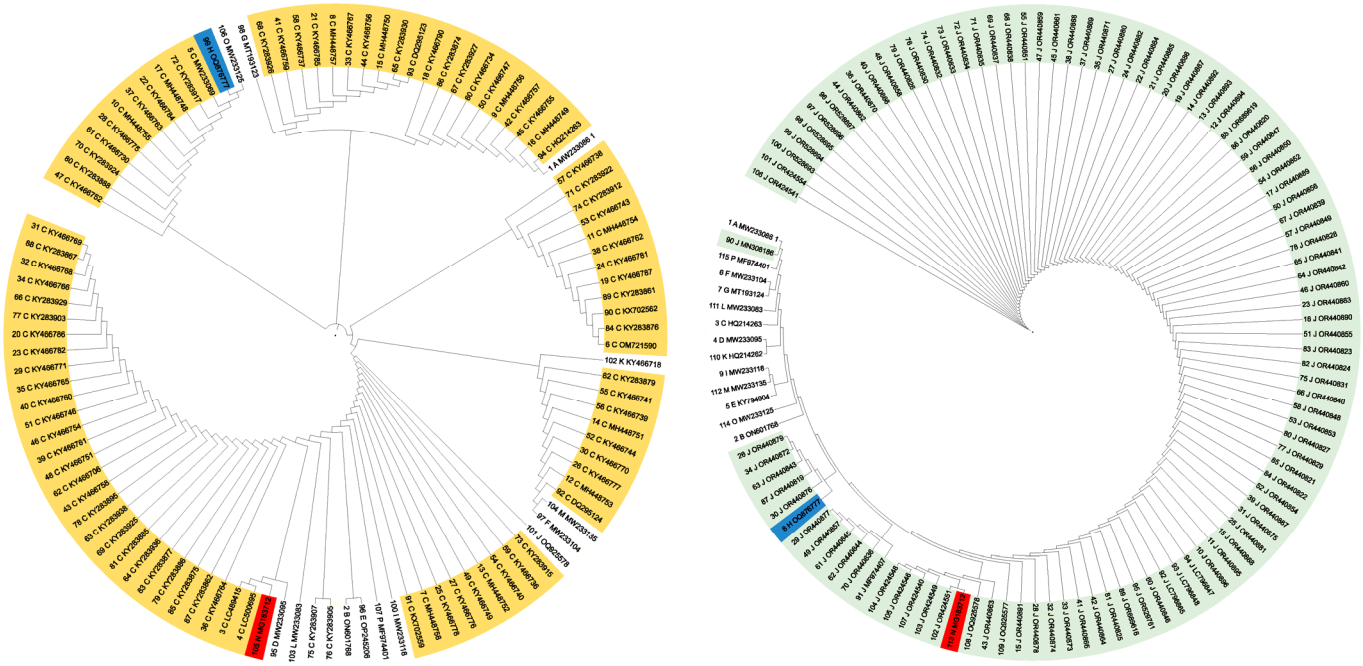

(**A**) (**B**)

Figure 1. *F. asiaticum* (**A**) and *Fgss* (**B**) NJ dendrograms. Yellow, green, blue, and red lines are predicting *F. asiaticum*, *Fgss*, *F. culmorum*, and *F. solani* samples, respectively.

It seems that NJ-based phylogenetics that included all samples (Set III) provided the closest distribution to the predicted systematic knowledge. *Fgss* samples showed a homogenous distribution in comparison to *F. asiaticum* samples. Hafez et al. (2020) [24] reposted similar co-clustering of *Fgss* isolates among nine FGSC members, eight FHB and/or CR agents, and *F. oxysporum* (as an outer group). In addition to developing a PCR-RFLP-based identification tool for FGSC members, they revealed that *Fgss* had a clearly distinct distribution from the remaining *Fusarium* spp. isolates. Similar results were also obtained for NJ-based topology analysis in Fgss isolates previously [17,25]. Overall, it

seems that NJ-based phylogenetic analysis would be useful for comprehensive phylogenetic analysis with a high number of samples among FGSC members, especially for *Fgss*.

The UPGMA dendrogram for Set I produced a nearly homogenous distribution for *F. asiaticum* samples within only one cluster. Two clusters were obtained, and division-II contained 80% of *F. asiaticum* samples, while division-I contained 20% of *F. asiaticum* samples, and the remaining FGSC members had *F. solani* (Figure 2A). Similar results were obtained for the UPGMA dendrogram for Set II (Figure 2B). 84% of *Fgss* samples were co-clustered in division I, and the remaining samples were included in the same division. *F. solani* seems to be the most genetically distinct sample for UPGMA analysis. Four major divisions were present in the UPGMA analysis for Set III. The majority of the *Fgss* and *F. asiaticum* samples were clearly located in separate divisions, which are closely related to each other (Figure S2). While all *F. meridionale* samples co-clustered in a single division, the remaining members of *F. solani* were distinct from the remaining isolates.

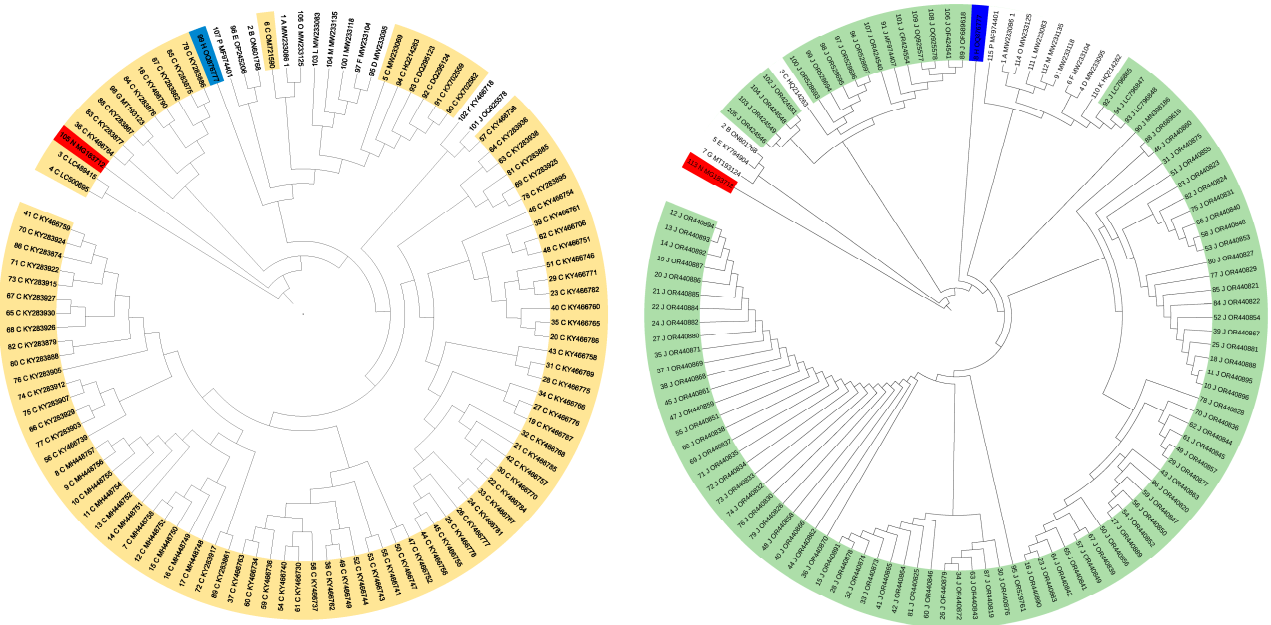

(**A**) (**B**)

Figure 2. *F. asiaticum* (**A**) and *Fgss* (**B**) UPGMA dendrograms. Yellow, green, blue, and red lines are predicting *F. asiaticum*, *Fgss*, *F. culmorum*, and *F. solani* samples, respectively.

UPGMA analysis yielded an almost homogenous distribution in FGSC members for three. Additionally, it was shown that *F. solani* was clearly genetically distinct from the majority of FGSC members, which was expected based on previous investigations [26,27]. There was idiomorphic UPGMA profiling for Argentinian *Fgss* isolates and other FGSC members by *tef1*−*α* sequence alignment [28] (Alvarez et al., 2011). It was reported that *Fgss* and *F. cortaderiae* precisely co-clustered in the same sub-division via the UPGMA method, and *F. culmorum* was genetically more closely related to *F. culmorum* in comparison to the non-FHB and CR pathogen *F. oxysporum* [29]. Our results showed a similar pattern of homogenous (but not idiomorphic) distribution among FGSC members, especially for *Fgss* and *F. asiaticum* isolates via UPGMA profiling. Moreover, the UPGMA method provided clear distinguishing between *F. boothii* and *F. meridionale* isolates.

3.2. Character-Based Phylogenetic Analysis

Iqtree software-based ML assays yielded best-fit models as TN + F + R2, TIM2e + G4, and TNe + R2 for Set I, Set II, and Set III, respectively. For each set, the p values and df values were recorded as follows: $p < 0.05$ and df = 3 by the chi2 test (Table 2). The maximum parsimony informative site was detected in Set I with a relatively minimum gap percentage. In the

ML-dendrogram of Set I, only two samples were distinctly clustered from *F. asiaticum* samples. *F. solani*, *F. culmorum*, and FGSC members but not *F. asiaticum* samples were co-clustered (Figure 3A). A similar clustering profile was obtained by ML analysis in Set II. The largest division included all Fgss samples, excluding one (Figure 3B). The smaller division included the remaining FGSC members with *F. culmorum* and *F. solani* samples. The ML dendrogram clearly distinguished *Fgss* and *F. asiaticum* samples from *F. boothii*, *F. meridionale*, and the remaining FGSC members. In addition, *F. solani* and *F. culmorum* samples were co-clustered, being located quite far from the *Fgss* and *F. asiaticum* samples (Figure S3).

Table 2. Alignment results obtained from iqtree-based ML treatment for three sets.

Set	Parsimony Informative Sites	Singleton Sites	Constant Sites	Gap/Ambiguity	Chi2 Test	Base Frequencies (A/C/G/T)
Set I	246	120	405	18.13%	$p < 0.05$, df = 3	0.220/0.301/0.220/0.259
Set II	36	158	554	20.38%	$p < 0.05$, df = 3	0.25/0.25/0.25/0.25
Set III	293	124	344	19.73%	$p < 0.05$, df = 3	0.25/0.25/0.25/0.25

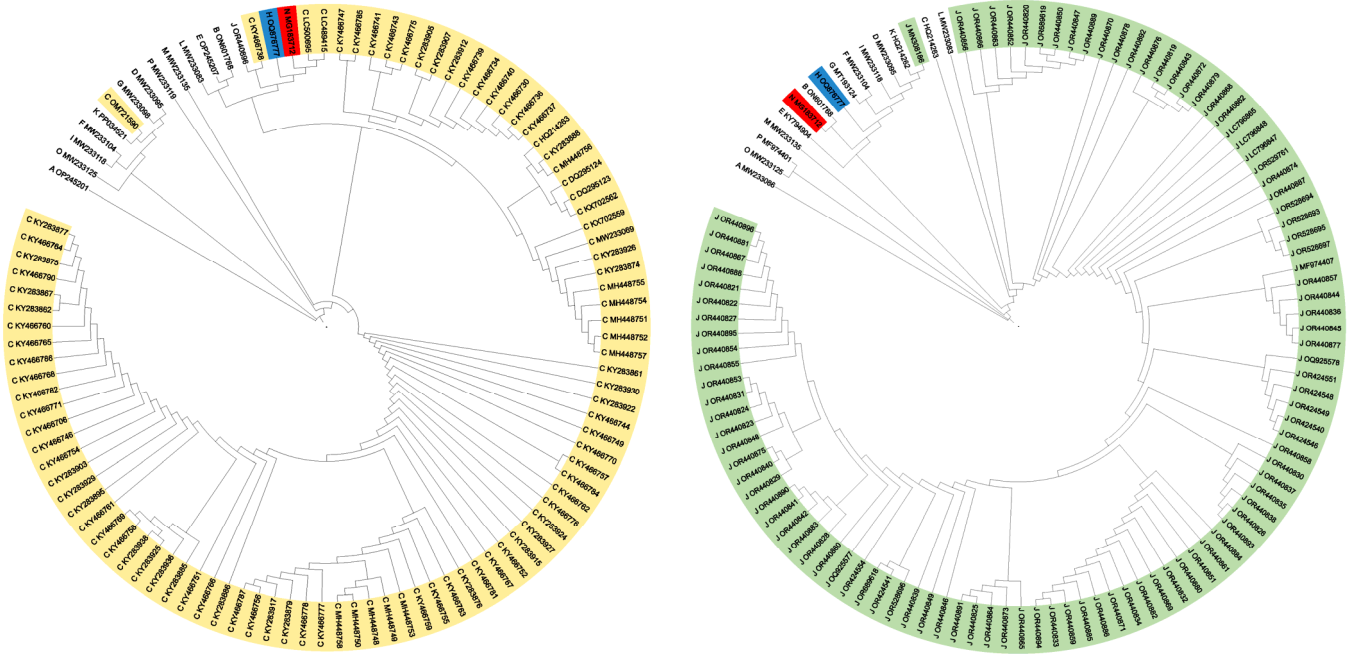

(**A**) (**B**)

Figure 3. *F. asiaticum* (**A**) and *Fgss* (**B**) ML dendrograms. Yellow, green, blue, and red lines are predicting *F. asiaticum*, *Fgss*, *F. culmorum*, and *F. solani* samples, respectively.

ML-based phylogenetic analysis provided effective distinction among FGSC members in terms of intraspecific variation. Especially, the location of the *F. solani* sample was clearly informative and distinguishable from the FHB and CR causal agents' *tef1*−*α* sequences. Similar ML profiling for FGSC members was present in previous studies [30,31]. *Fgss*, *F. meridionale*, *F. asiaticum*, and *F. boothii* isolates from Iraq, Poland, and Austria were clearly distinguished from *Fusarium* spp. isolates not related to FHB and CR. Overall, it could be concluded that ML-based phylogenetic analysis could provide reliable characterization and clustering of *Fgss* and *F. asiaticum* isolates from FGSC members.

Bayesian phylogenetics were obtained by using MrBayes software. Bayesian topology yielded not more than two divisions for all three sets (Figure 4A,B). However, Bayesian dendrograms for Set I and Set II clearly showed distinct clustering of *F. solani* and *F. culmorum* samples from *F. asiaticum* and *Fgss* samples, respectively (Figure 4A,B). Set III dendrogram provided heterogeneous distribution of *F. asiaticum* and *Fgss* samples among

the largest division. Even if *F. meridionale* and *F. boothii* samples were located between the majority of *Fgss* and *F. asiaticum* samples, as in distance-based Set III dendrograms, 6 *F. asiaticum* and 4 *Fgss* samples clustered apart from the majority of Set I and Set II samples (Figure S4). In comparison to the remaining three phylogenetic analysis methods, Bayesian topology would be more useful in member-specific alignment analysis due to the heterogeneous distribution of *F. asiaticum* and *Fgss* samples in Set III.

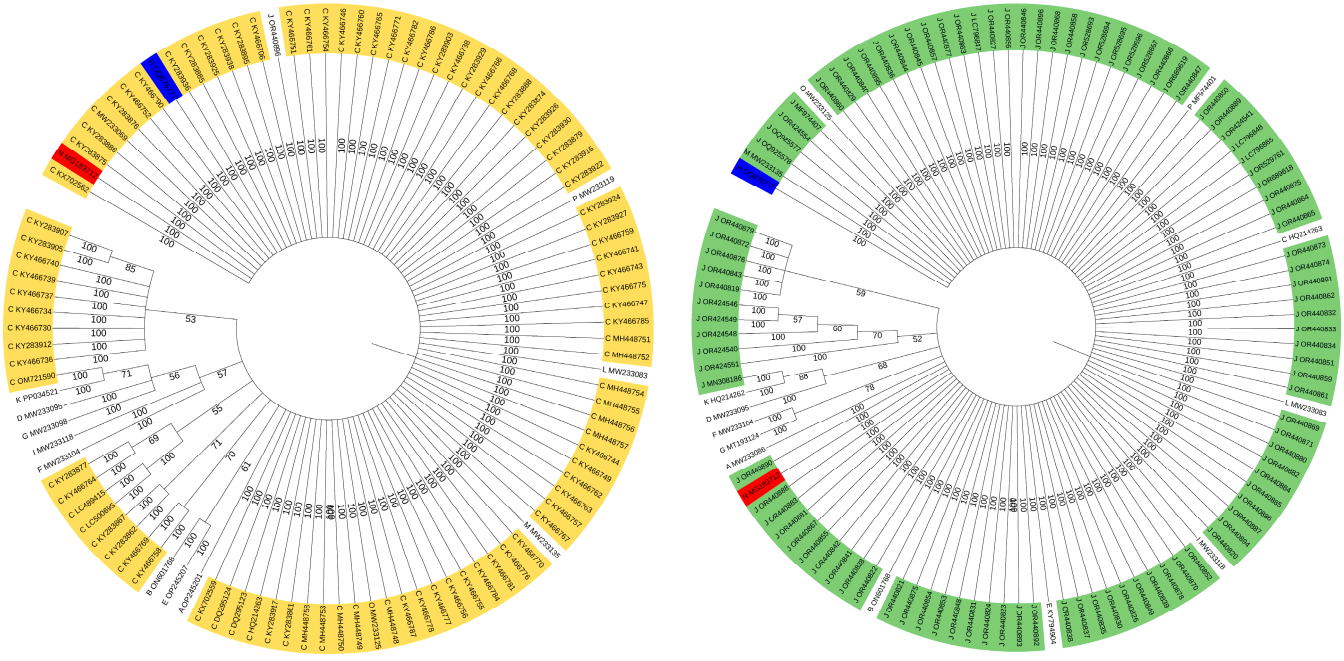

(**A**) (**B**)

Figure 4. *F. asiaticum* (**A**) and *Fgss* (**B**) Bayesian dendrograms. Yellow, green, blue, and red lines are predicting *F. asiaticum*, *Fgss*, *F. culmorum*, and *F. solani* samples, respectively.

To our knowledge, there is no present, detailed investigation for FGSC phylogenetic analysis via Bayesian topology. Several *Fusarium* spp. species excluding FGSC members have been identified and characterized by multiple alignment assays combined with Bayesian topology in the *tef1*−*α*, *tub2*, *cyp51C*, and *rpb2* genes [32–34]. Similar to the existing studies, including Bayesian topology analysis for *Fusarium* spp., homogenous distributions of *Fusarium* spp. isolates belonging to the same species were present in this study.

3.3. PCA-Based Similarity Analysis

PCA tests were carried out using the R programming language for three sets separately. Set I PCA revealed 99.5% and 0.4% percentages for dimension 1 and dimension 2, respectively (Figure 5A). The *F. solani* isolate with accession number N_MG183712 was clearly located a quite far away from the FHB and CR causal agents. Additionally, two *F. asiaticum* samples (C_LC489415 and C_LC500695) were not co-clustered with the remaining 90 *F. asiaticum* samples. In comparison to the Set I PCA graphic, Set II samples were regularly clustered within dimension I (99.3%). Similarly, the *F. solani* isolate was clustered distinctively from all FHB and CR pathogens (Figure 5B). Set III revealed a natural combination of PCA graphics from Set I and Set II in terms of the homogenous distribution of FHB and CR pathogens with a 99.5% percentage of dimension 1 (Figure S5). PCA profiling of three different sets produced an overall homogenous distribution of FGSC members via *tef1*−*α* sequence alignment analysis.

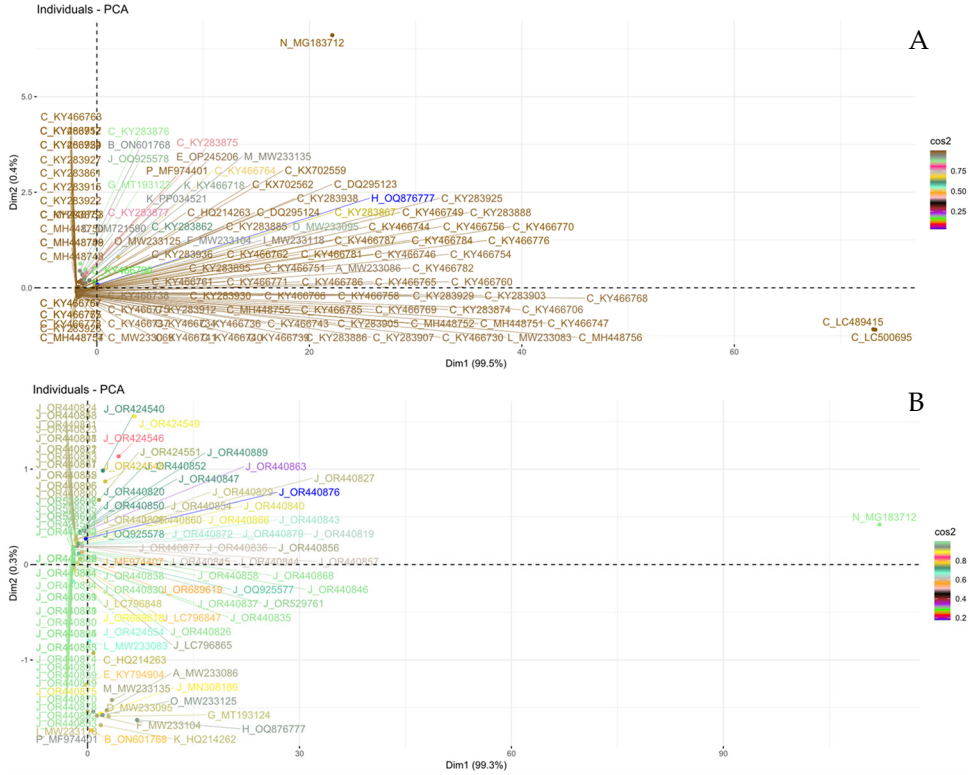

Figure 5. PCA profiling of *F. asiaticum* (**A**) and *Fgss* (**B**) samples subjected to *tef1*−*α* sequence based phylogenetic analysis.

Distance-based methods and character-based methods revealed strong co-clustering of *Fgss* and *F. asiaticum* isolates from remaining FGSC members, *F. culmorum*, and *F. solani*. Phylogenetic analysis for especially Set III resulted in FGSC members clustering in different sub-divisions from non-FHB and non-CR pathogens, as reported previously [17,24,25,28–31]. Especially UPGMA-based phylogenetics resulted in a homogenous distribution of *Fgss* and *F. asiatium* isolates. Similar data were obtained from ML-based phylogenetic analysis. *Fgss* and *F. asiaticum* isolates co-clustered in separate sub-divisions from the remaining FGSC members, *F. culmorum* and *F. solani*. Even if UPGMA has some limitations, such as assuming the same evolutionary speed and evolution rate, our results showed that UPGMA would be useful in phylogenetic studies that include a high number of samples with a limited number of taxa [35,36]. Similarly, ML-based phylogenetic analysis resulted in a great level of distinction between *Fgss* and *F. asiaticum* isolates from other *Fusarium* spp. This success in ML-phylogenetics in FGSC characterization might be due to the fact that there was no outlier or genetically most distant sample presence in the aligned data [37,38]. In addition to UPGMA- and ML-based phylogenetics, PCA also seemed to be an effective strategy for revealing the homogenous distribution of *F. asiaticum*, *Fgss*, *F. meridionale*, and *F. boothii*. FGSC members were clustered together in PCA profiling, resulting in a 99.5% percentage of homology. Phylogenetic analysis approaches supported by PCA tests are particularly important for increasing the reliability of studies of fungal species where subspecies or species complexes exist. PCA tests offer a holistic approach when compared to phylogenetic tests based on different mathematical arguments and help to clearly identify individuals at the genetic level when the phylogenetic diagnosis is in doubt. In this content, these results showed that FGSC members could effectively be genetically characterized via UPGMA- and ML-based phylogenetics in *tef1*−*α* sequence alignment strategies.

4. Conclusions

F. graminearum has always been at the center of interest for those studying plant pathology. Its global distribution, capacity to produce different types of important myco-

toxins, being a species complex with geographically confusing distribution, and some other characteristics made *F. graminearum* such a popular phytopathogenic fungus worldwide. However, the need for the precise identification of FGSC members (formerly named as lineage) led scientists to develop reliable and verifiable methods. Hitherto, it is safe to say that multilocus genotyping has met this need. However, it could be concluded that *tef1−α* sequencing has also been quite successful on its own. This study was designed, in a sense, to test the success of the genetic identification of FGSC members by *tef1−α* sequencing. Four different methods were used for phylogenetic analysis with 246 FGSC members. Even if NJ and Bayesian topology assays revealed a relatively heterogeneous distribution of *F. solani* and *F. culmorum* within sub-divisions of FGSC members, the majority of *Fgss* and *F. asiaticum* isolates co-clustered in two large sub-divisions. The UPGMA and ML methods, which provided a near-perfect FGSC member characterization, were validated by PCA. The results showed that especially UPGMA- and ML-based phylogenetic treatments in FGSC members would be useful in member-specific genetic characterization via *tef1−α* sequencing data. This is also the first study to combine phylogenetic methods with PCA tests to reveal member-specific characterization in FGSC. An increased number of taxa with a higher number of FGSC isolates would be tested by using character- and distance-based phylogenetic analysis for *tef1−α* in future studies.

Supplementary Materials: The following supporting information can be downloaded at: https://www.mdpi.com/article/10.3390/d16080481/s1: Figure S1: NJ dendrogram for 248 *Fusarium* spp. Isolates. Yellow, green, blue, red, purple, and gray lines are predicting *F. asiaticum*, *Fgss*, *F. culmorum*, *F. solani*, *F. meridionale*, and *F. boothii* samples, respectively. Figure S2: UPGMA dendrogram for 248 *Fusarium* spp. Isolates. Yellow, green, blue, red, purple, and gray lines are predicting *F. asiaticum*, *Fgss*, *F. culmorum*, *F. solani*, *F. meridionale*, and *F. boothii* samples, respectively. Figure S3: ML dendrogram for 248 *Fusarium* spp. Isolates. Yellow, green, blue, red, purple, and gray lines are predicting *F. asiaticum*, *Fgss*, *F. culmorum*, *F. solani*, *F. meridionale*, and *F. boothii* samples, respectively. Figure S4: Bayesian topology dendrogram for 248 *Fusarium* spp. Isolates. Yellow, green, blue, red, purple, and gray lines are predicting *F. asiaticum*, *Fgss*, *F. culmorum*, *F. solani*, *F. meridionale*, and *F. boothii* samples, respectively. Figure S5: PCA profiling for 248 *Fusarium* spp. isolates.

Author Contributions: Conceptualization, E.Y. and T.Y.-M.; methodology, E.Y.; software, E.Y.; validation, E.Y. and T.Y.-M.; formal analysis, E.Y. and T.Y.-M.; investigation, E.Y. and T.Y.-M.; resources, E.Y. and T.Y.-M.; data curation, E.Y. and T.Y.-M.; writing—original draft preparation, E.Y.; writing—review and editing, T.Y.-M.; visualization, E.Y. and T.Y.-M.; supervision, T.Y.-M.; project administration, E.Y.; funding acquisition, E.Y. All authors have read and agreed to the published version of the manuscript.

Funding: This research received no external funding.

Institutional Review Board Statement: Not applicable.

Data Availability Statement: The DNA sequence data subjected to phylogenetic analysis in this study are deposited under the accession number given in Table 1.

Conflicts of Interest: The authors declare no conflicts of interest.

References

1. McMullen, M.; Jones, R.; Gallenberg, D. Scab of Wheat and Barley: A Re-emerging Disease of Devastating Impact. *Plant Dis.* **1997**, *81*, 1340–1348. [CrossRef] [PubMed]
2. Parry, D.W.; Jenkinson, P.; McLE, L. Fusarium ear blight (scab) in small grain cereals—A review. *Plant Pathol.* **1995**, *44*, 207–238. [CrossRef]
3. Yli-Manila, T.; Gagkaeva, T.Y. Fusarium toxins in cereals in northern Europe and Asia. In *Fungi*; CRC Press: Boca Raton, FL, USA, 2018; pp. 293–317.
4. Desjardins, A.E. Fusarium Mycotoxins: Chemistry, Genetics, and Biology. 2006. Available online: https://www.cabidigitallibrary.org/doi/full/10.5555/20063036927 (accessed on 14 July 2024).
5. Desjardins, A.E.; Proctor, R.H. Molecular biology of Fusarium mycotoxins. *Int. J. Food Microbiol.* **2007**, *119*, 47–50. [CrossRef] [PubMed]

6. Dean, R.; Van Kan, J.A.L.; Pretorius, Z.A.; Hammond-Kosack, K.E.; Di Pietro, A.; Spanu, P.D.; Rudd, J.J.; Dickman, M.; Kahmann, R.; Ellis, J.; et al. The Top 10 fungal pathogens in molecular plant pathology. *Mol. Plant Pathol.* **2012**, *13*, 414–430. [CrossRef] [PubMed]
7. O'donnell, K.; Humber, R.A.; Geiser, D.M.; Kang, S.; Park, B.; Robert, V.A.R.G.; Crous, P.W.; Johnston, P.R.; Aoki, T.; Rooney, A.P.; et al. Phylogenetic diversity of insecticolous fusaria inferred from multilocus DNA sequence data and their molecular identification via FUSARIUM-ID and Fusarium MLST. *Mycologia* **2012**, *104*, 427–445. [CrossRef] [PubMed]
8. Nicholson, P.; Chandler, E.; Draeger, R.C.; Gosman, N.E.; Simpson, D.R.; Thomsett, M.; Wilson, A.H. Molecular tools to study epidemiology and toxicology of Fusarium head blight of cereals. *Eur. J. Plant Pathol.* **2003**, *109*, 691–703. [CrossRef]
9. Schilling, A. Polymerase chain reaction-based assays for species-specific detection of *Fusarium culmorum*, *F. graminearum*, and *F. avenaceum*. *Phytopathology* **1996**, *86*, 515–522. [CrossRef]
10. Zhang, X.; Ma, H.; Zhou, Y.; Xing, J.; Chen, J.; Yu, G.; Sun, X.; Wang, L. Identification and Genetic Division of *Fusarium graminearum* and *Fusarium asiaticum* by Species-Specific SCAR Markers. *J. Phytopathol.* **2014**, *162*, 81–88. [CrossRef]
11. O'Donnell, K.; Kistler, H.C.; Tacke, B.K.; Casper, H.H. Gene genealogies reveal global phylogeographic structure and reproductive isolation among lineages of *Fusarium graminearum*, the fungus causing wheat scab. *Proc. Natl. Acad. Sci. USA* **2000**, *97*, 7905–7910. [CrossRef]
12. O'Donnell, K.; Sarver, B.A.J.; Brandt, M.; Chang, D.C.; Noble-Wang, J.; Park, B.J.; Sutton, D.A.; Benjamin, L.; Lindsley, M.; Padhye, A.; et al. Phylogenetic Diversity and Microsphere Array-Based Genotyping of Human Pathogenic Fusaria, Including Isolates from the Multistate Contact Lens-Associated U.S. Keratitis Outbreaks of 2005 and 2006. *J. Clin. Microbiol.* **2007**, *45*, 2235–2248. [CrossRef]
13. O'donnell, K.; Ward, T.J.; Aberra, D.; Kistler, H.C.; Aoki, T.; Orwig, N.; Kimura, M.; Bjørnstad, S.; Klemsdal, S.S. Multilocus genotyping and molecular phylogenetics resolve a novel head blight pathogen within the *Fusarium graminearum* species complex from Ethiopia. *Fungal Genet. Biol.* **2008**, *45*, 1514–1522. [CrossRef] [PubMed]
14. Sarver, B.A.J.; Ward, T.J.; Gale, L.R.; Broz, K.; Kistler, H.C.; Aoki, T.; Nicholson, P.; Carter, J.; O'donnell, K. Novel Fusarium head blight pathogens from Nepal and Louisiana revealed by multilocus genealogical concordance. *Fungal Genet. Biol.* **2011**, *48*, 1096–1107. [CrossRef] [PubMed]
15. Wang, C.; Zhang, S.; Hou, R.; Zhao, Z.; Zheng, Q.; Xu, Q.; Zheng, D.; Wang, G.; Liu, H.; Gao, X.; et al. Functional analysis of the kinome of the wheat scab fungus *Fusarium graminearum*. *PLoS Pathog.* **2011**, *7*, e1002460. [CrossRef] [PubMed]
16. Garmendia, G.; Umpierrez-Failache, M.; Ward, T.J.; Vero, S. Development of a PCR-RFLP method based on the transcription elongation factor 1-gene to differentiate *Fusarium graminearum* from other species within the *Fusarium graminearum* species complex. *Food Microbiol.* **2018**, *70*, 28–32. [CrossRef] [PubMed]
17. Tunal, B.; Yrk, E.; Sefer, Ö.; Kansu, B.; Sharifnabi, B. First Report on Identification of *Fusarium graminearum* Species Complex Members from Turkey and Iran. *Turk. J. Agric. Food Sci. Technol.* **2019**, *7*, 1040–1045. [CrossRef]
18. Qu, B.; Li, H.P.; Zhang, J.B.; Huang, T.; Carter, J.; Liao, Y.C.; Nicholson, P. Comparison of genetic diversity and pathogenicity of fusarium head blight pathogens from China and Europe by SSCP and seedling assays on wheat. *Plant Pathol.* **2008**, *57*, 642–651. [CrossRef]
19. Wang, C.-L.; Cheng, Y.-H. Identification and trichothecene genotypes of *Fusarium graminearum* species complex from wheat in Taiwan. *Bot. Stud.* **2017**, *58*, 4. [CrossRef]
20. Yörük, E.; Albayrak, G. Genetic characterization of *Fusarium graminearum* and *F. culmorum* isolates from Turkey by using random-amplified polymorphic DNA. *Genetics and Molecular Research* **2013**, *12*, 1360–1372. [CrossRef] [PubMed]
21. Letunic, I.; Bork, P. Interactive Tree of Life (iTOL) v6: Recent updates to the phylogenetic tree display and annotation tool. *Nucleic Acids Res.* **2024**, *52*, 78–82. [CrossRef]
22. Nguyen, L.-T.; Schmidt, H.A.; Von Haeseler, A.; Minh, B.Q. IQ-TREE: A fast and effective stochastic algorithm for estimating maximum-likelihood phylogenies. *Mol. Biol. Evol.* **2015**, *32*, 268–274. [CrossRef]
23. Huelsenbeck, J.P.; Ronquist, F. MRBAYES: Bayesian inference of phylogenetic trees. *Bioinformatics* **2001**, *17*, 754–755. [CrossRef] [PubMed]
24. Hafez, M.; Abdelmagid, A.; Adam, L.R.; Daayf, F. Specific Detection and Identification of *Fusarium graminearum* Sensu Stricto Using a PCR-RFLP Tool and Specific Primers Targeting the Translational Elongation Factor 1α Gene. *Plant Dis.* **2020**, *104*, 1076–1086. [CrossRef] [PubMed]
25. Boutigny, A.-L.; Gautier, A.; Basler, R.; Dauthieux, F.; Leite, S.; Valade, R.; Aguayo, J.; Ioos, R.; Laval, V. Metabarcoding targeting the EF1 alpha region to assess Fusarium diversity on cereals. *PLoS ONE* **2019**, *14*, e0207988. [CrossRef] [PubMed]
26. Geiser, D.M.; Aoki, T.; Bacon, C.W.; Baker, S.E.; Bhattacharyya, M.K.; Brandt, M.E.; Brown, D.W.; Burgess, L.W.; Chulze, S.; Coleman, J.J.; et al. One Fungus, One Name: Defining the Genus Fusarium in a Scientifically Robust Way That Preserves Longstanding Use. *Phytopathology* **2013**, *103*, 400–408. [CrossRef] [PubMed]
27. Geiser, D.M.; Al-Hatmi, A.M.S.; Ao, T.; Arie, T.; Balmas, V.; Barnes, I.; Viljoen, A. Phylogenomic Analysis of a 55. 1-kb 19-Gene Dataset Resolves a Monophyletic *Fusarium* that Includes the *Fusarium solani* Species Complex. *Phytopathology* **2021**, *111*, 1064–1079. [CrossRef] [PubMed]
28. Alvarez, C.L.; Somma, S.; Proctor, R.H.; Stea, G.; Mulè, G.; Logrieco, A.F.; Pinto, V.F.; Moretti, A. Genetic Diversity in *Fusarium graminearum* from a Major Wheat-Producing Region of Argentina. *Toxins* **2011**, *3*, 1294–1309. [CrossRef] [PubMed]

29. Bentley, A.R.; Cromey, M.G.; Farrokhi-Nejad, R.; Leslie, J.F.; Summerell, B.A.; Burgess, L.W. *Fusarium* crown and root rot pathogens associated with wheat and grass stem bases on the South Island of New Zealand. *Australas. Plant Pathol.* **2006**, *35*, 495. [CrossRef]
30. Minati, M.H.; Mohammed-Ameen, M.K. Novel report on six Fusarium species associated with head blight and crown rot of wheat in Basra province, Iraq. *Bull. Natl. Res. Cent.* **2019**, *43*, 139. [CrossRef]
31. Stępniewska, H.; Jankowiak, R.; Bilański, P.; Hausner, G. Structure and Abundance of Fusarium Communities Inhabiting the Litter of Beech Forests in Central Europe. *Forests* **2021**, *12*, 811. [CrossRef]
32. Fernández-Ortuño, D.; Loza-Reyes, E.; Atkins, S.L.; Fraaije, B.A. The CYP51C gene, a reliable marker to resolve interspecific phylogenetic relationships within the Fusarium species complex and a novel target for species-specific PCR. *Int. J. Food Microbiol.* **2010**, *144*, 301–309. [CrossRef]
33. Noel, Z.A.; Roze, L.V.; Breunig, M.; Trail, F. Endophytic Fungi as a Promising Biocontrol Agent to Protect Wheat from *Fusarium graminearum* Head Blight. *Plant Dis.* **2022**, *106*, 595–602. [CrossRef]
34. Sanna, M.; Martino, I.; Guarnaccia, V.; Mezzalama, M. Diversity and Pathogenicity of Fusarium Species Associated with Stalk and Crown Rot in Maize in Northern Italy. *Plants* **2023**, *12*, 3857. [CrossRef] [PubMed]
35. Backeljau, T.; De Bruyn, L.; De Wolf, H.; Jordaens, K.; Van Dongen, S.; Winnepennincks, B. Multiple UPGMA and Neighbor-joining Trees and the Performance of Some Computer Packages. *Mol. Biol. Evol.* **1996**, *13*, 309–313. [CrossRef]
36. Drummond, A.; Rodrigo, A.G. Reconstructing Genealogies of Serial Samples Under the Assumption of a Molecular Clock Using Serial-Sample UPGMA. *Mol. Biol. Evol.* **2000**, *17*, 1807–1815. [CrossRef]
37. Michu, E. A short guide to phylogeny reconstruction. *Plant Soil Environ.* **2007**, *53*, 442–446. [CrossRef]
38. Saitou, N. Property and efficiency of the maximum likelihood method for molecular phylogeny. *J. Mol. Evol.* **1988**, *27*, 261–273. [CrossRef]

Disclaimer/Publisher's Note: The statements, opinions and data contained in all publications are solely those of the individual author(s) and contributor(s) and not of MDPI and/or the editor(s). MDPI and/or the editor(s) disclaim responsibility for any injury to people or property resulting from any ideas, methods, instructions or products referred to in the content.